Jpn. J. Appl. Phys. Vol. 35 (1996) pp. L 731–L 734
Part 2, No. 6A, 1 June 1996

Dynamic Formation of Excited Helicon Wave Structure and Estimation of Wave Energy Flux Distribution

Shunjiro SHINOHARA*, Yoko MIYAUCHI and Yoshinobu KAWAI
Interdisciplinary Graduate School of Engineering Science, Kyushu University, Kasuga, Fukuoka 816, Japan

(Received February 29, 1996; accepted for publication April 8, 1996)

Dynamic changes in helicon wave structure, due to excitation by a helical antenna, are investigated as a function of time. Before a density jump (steep density increase), not a propagating wave but a standing wave near the antenna is found. After the jump, a selective helicon wave excitation of azimuthal mode numbers $m = 1$ and $m = -1$ is demonstrated, and the first the energy flux estimate shows different axial profiles for the two modes.

KEYWORDS: RF plasma, helicon wave, wave structure, helical antenna, energy flux

A helicon wave[1-10] has been recognized as an effective high-density plasma source for plasma processing linear devices as well as for toroidal confinement ones. Although a high-density plasma up to $\leq 10^{13}$ cm^{-3} can be produced by an application of RF waves with axial magnetic field of more than several hundreds of G, there are only a few basic studies on helicon wave phenomena: most measured radial wave field profiles[1,4,5,7,8] do not agree well with theoretical profiles, and only azimuthal mode number $m = 1$ (the plus sign indicates right - hand circular polarization) could be excited in spite of the various antenna configurations tried.[8] The time evolution of excited wave patterns along the axial length and the dispersion relation[9] was investigated and shows a helicon wave character after a density jump (abrupt density increase to a level of 10^{13} cm^{-3}). However, studies concerning the change of wave fields, comparing with the theoretical expected profiles of the helicon wave, have not been reported, and the wave energy flux distribution, which can be a clue to clarify the wave damping mechanism related to the plasma production, has not been measured. In this letter, we describe experimental studies on dynamic helicon wave formation by measuring the excited wave fields. The time evolution of radial and axial profiles of wave fields (amplitude and phase) are measured, and we show an estimation of the wave energy flux (Poynting vector) along the axial length for the first time.

The experiments have been carried out for a conventional linear device.[9] The source is a Pyrex tube (inner diameter is 5 cm and total length is 50 cm (axial position of $z = -35 \sim 15$ cm)), which is connected to an expanded vacuum chamber, and the antenna length is 20 cm ($z = -20 \sim 0$ cm) and has one-turn helical winding. The pressure of Ar gas near the pump head is 0.6 mTorr with the static axial magnetic field of 1 kG. The RF input power and frequency are 1–2 kW and 7 MHz, respectively, and the RF pulse width is 2 ms with a duty of < 0.1. Exciting $m = 1$ or -1 azimuthal modes can be selected by changing the sign of the axial magnetic field, as long as a wave reflected in the other direction is neglected. Typical electron temperature and density after the density jump are in the ranges of 3–10 eV and 10^{13}–10^{14} cm^{-3}, respectively. The excited wave fields are measured using movable magnetic probes (one-turn coil with ± 2 mm resolution) inserted into the plasma. A balanced mixer for the interferometric wave measurements and a boxcar integrator are also used.

Figure 1 shows the time evolution of radial profiles of the excited magnetic fields of three components (B_r, B_θ and B_z components in the cylindrical geometry) for $m = 1$ excitation at $z = 23$ cm from the right edge of the antenna. These fields are measured using the interferometric method with the RF generator signal, and one example of theoretical expected fields for the case of the parabolic density profile[6] is also shown (in which plasma and wall radii are 5 cm, wavelength is 24 cm and wave frequency is 27.12 MHz). For convenience, we indicate that the amplitude is positive at r slightly larger than zero. At the initial phase of the RF pulse at $t = 0.1$ ms, all three components are nearly in phase with each other and show broad profiles, which are neither expected from the helicon wave profiles (see Fig. 1(d)), nor from the vacuum field ones excited by the antenna current.[5] During the plasma formation phase at $t = 0.3$ ms, a more peaked

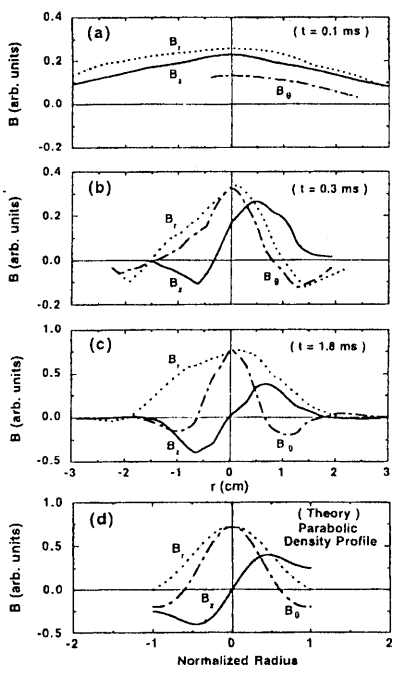

Fig. 1. Radial profiles of magnetic fields measured by interferometric method at (a) $t = 0.1$ ms, (b) $t = 0.3$ ms and (c) $t = 1.8$ ms, and (d) calculated fields[6] for $m = 1$ excitation.

*E-mail address: shinoigh@mbox.nc.kyushu-u.ac.jp

profile is observed, which exhibits an asymmetric profile of the B_z component. After that time (well after the density jump phase, at $t > 1$ ms), magnetic field profiles become almost unchanging, as shown in Fig. 1(c), at $t = 1.8$ ms. These profiles are in fairly good agreement with one example of the expected profiles shown in Fig. 1(d), and the obtained phases between the three components are also consistent with the expectation, i.e., right-hand circular polarization.

Figure 2 shows radial profiles of the measured magnetic fields ($z = 23$ cm) at $t = 1$ ms and one example of a theoretically expected field for the parabolic density profile[6] for $m = -1$ excitation. Note that we measure magnetic field profiles at the time when amplitudes of B_r and B_θ at the plasma center are slightly different in one RF cycle. As for the $m = 1$ excitation, after taking broad and then transient (asymmetry) profiles, nearly steady profiles (see Fig. 2 (a) at $t = 1$ ms) are obtained which agree well with one example of the theoretical expectation, and a left-hand circular polarization is confirmed from the phase measurements. Theoretically, the maximum amplitude of the B_z field is smaller (larger) than the amplitudes of B_r and B_θ at the plasma center for $m = 1$ ($m = -1$) excitation. This trend (and also the shrinkage of the wave profile itself) is more pronounced with an increase in the sharpness of the density peak, which is consistent with the experimental results, as shown in Figs. 1 and 2. These results of the obtained field profiles shown in Figs. 1 and 2 (and also the polarization directions) well after the density jump, compared with the theoretical results, show that we can demonstrate the selective excitation of $m = 1$ and $m = -1$ modes in our experiments, contrary to the results obtained by another group,[8] in which only the $m = 1$ mode could be excited. The different results may mainly be due to 1) lower pressure and higher plasma density, 2) higher selectivity of the exciting helical current mode because of the use of one-turn instead of half-turn antennae, and 3) different boundary conditions (Pyrex tube and expanded stainless vacuum chamber in our case) compared with the experimental conditions in ref. 8.

Figures 3 and 4 show axial profiles of the phase $\Delta\phi$ and effective amplitude $B_\perp$ of the excited wave (plasma center) at $t = 0.03$ ms (before the density jump) and at $t = 1.8$ ms (after the density jump), respectively, for $m = 1$ and -1 excitations. Here, $\Delta\phi$ is taken between the measured antenna current and $B_\perp$ (perpendicular component). At $t = 0.03$ ms $\Delta\phi$ changes smoothly with the z axis near the antenna region (magnetic field amplitude is large) and is nearly constant in the outside region (amplitude is smaller by more than one order of magnitude) for both excitations. After this time the relative amplitude in the outside antenna region increases with time for $m = 1$ excitation and increases slightly for $m = -1$ excitation. The boundary of changing phase shifts to the right with time, beyond the edge (right side) of the antenna along the z axis for both excitations, and the constant phase region finally disappears. Although standing wave behavior is still exhibited near the antenna, especially for $m = -1$ excitation at $t = 1.8$ ms, the phase of $\Delta\phi$ (and the amplitude for $m = 1$ excitation) is smoothly connected to the outer antenna region. Note that turning points ($z \sim -23$ cm for $m = 1$ and $z \sim -3$ cm for $m = -1$ excitation) of the phase correspond to the maximum amplitude position. Results from Figs. 3 and 4 support the previous observation,[9]

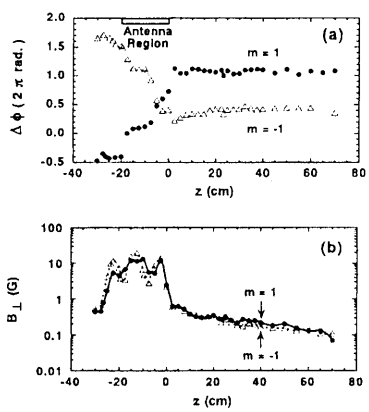

Fig. 3. Axial profiles of (a) wave phase $\Delta\phi$ and (b) perpendicular component of wave amplitude $B_\perp$ measured at $t = 0.03$ ms for $m = 1$ (closed circles) and $m = -1$ (open triangles) excitation.

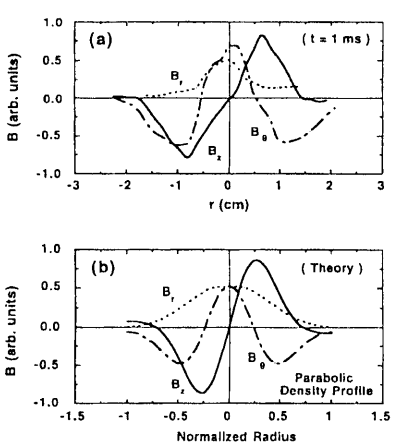

Fig. 2. Radial profiles of (a) magnetic fields measured by interferometric method at $t = 1$ ms, and (b) calculated fields[6] for $m = -1$ excitation.

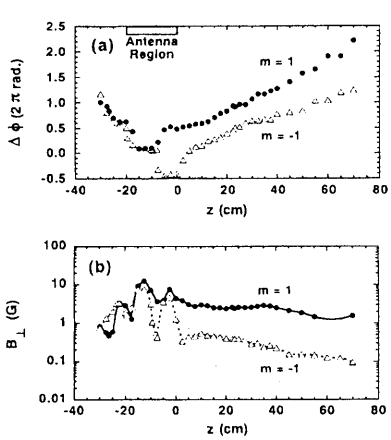

Fig. 4. Axial profiles of (a) wave phase $\Delta\phi$ and (b) perpendicular component of wave amplitude $B_\perp$ measured at $t = 1.8$ ms for $m = 1$ (closed circles) and $m = -1$ (open triangles) excitation.

showing a localized standing wave near the antenna without propagating to the outside region before the density jump, and a propagating helicon wave structure after the jump. In addition, a dispersion relation on the (plasma frequency, parallel wave number k_z) plane along the z direction roughly satisfies that of a helicon wave from the local measurements of k_z and n_e (electron density).

We try to estimate the energy flux distribution S_z along the z axis from the magnetic field data. The energy flux is the same as the Poynting flux, since the nonelectromagnetic energy flux due to coherent particle motion can be neglected.[10] If the E_z term is small compared with other components of E_r and E_θ, i.e., collisional and electron Landau damping rates are small, E_r and E_θ become $(\omega/k_z)\ B_\theta$ and $-(\omega/k_z)\ B_r$, respectively, using $\nabla\times E = -\partial B/\partial t$ (ω : excited wave angular frequency). Then the z direction of the Poynting vector can be written as follows.[10]

$$S_z = \frac{1}{2\mu_0}\left(\frac{\omega}{k_z}\right) Re(B_r^* B_r + B_\theta^* B_\theta) \qquad (1)$$

Here μ_0, asterisk and Re mean permeability in the vacuum, complex conjugate and real part, respectively. Note that B_r and B_θ can be expressed as a Bessel function if the density profile is flat.[2] A more general form of this Poynting vector[10] is

$$S_z = \frac{-\omega_{ce}}{2\mu_0}\left(\frac{c}{\omega_{pe}}\right)^2 Re\left(\frac{\partial B_z^*}{\partial r}B_\theta + \frac{im}{r}B_r B_z^*\right), \qquad (2)$$

where ω_{ce} and ω_{pe} are electron cyclotron and plasma frequencies, respectively. This formula holds even if the collisional and electron Landau damping cannot be neglected, as long as the excited wave satisfies the cold plasma dispersion relation with ω_{ci} (ion cyclotron frequency) $\ll \omega \ll \omega_{ce}$. In estimating $S_z(0)$ (plasma center), information about k_z and $B_\perp$ are necessary in eq. (1), and in eq. (2), n_e and the radial profile of the B_z component near the inner plasma region are also needed in addition.

Figure 5 shows the derived $S_z(0)$ as a function of z axis location at $t = 1.8$ ms for $m = 1$ and -1 excitations. Here, circles, diamonds and boxes show values derived from eq. (1) and triangles those derived from the general expression of eq. (2). Near the antenna region, a standing-wave-like phenomenon is observed, as shown in Fig. 4, which is considered as a mixture of right and left propagating helicon waves with nearly the same amplitude.[9] The upper (lower) diamond (box) symbols near the antenna region in Fig. 5 indicate the position of the maximum excited amplitude under an assumption that the wave propagating to the positive z direction has the full (one-half) observed amplitude. At $z \sim -10$ cm $S_z(0)$ may be close to the lower symbols, and the actual $S_z(0)$ near the antenna region takes an intermediate value between the upper and lower symbols. At the antenna region, the mean value of the initial energy flux is 46 W/cm^2 if defined as the net absorbed RF power[9] divided by two times of the plasma cross section. If we use eq. (1) from the magnetic field profile under an assumption of a parabolic density profile,[6] the initial energy flux at the plasma center $S_{zi}(0)$ becomes 277 (200) W/cm^2 for $m = 1$ (-1) excitation, which is consistent with the experimental value.

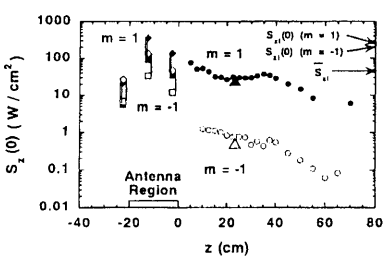

Fig. 5. Axial profiles of the Poynting vector $S_z(0)$ at $t = 1.8$ ms for $m = 1$ (closed symbols) and $m = -1$ (open symbols) excitations. Here, circles, diamonds and boxes show values derived from eq. (1) (boxes represent values obtained under the assumption of a standing wave), and triangles those derived from the general expression of eq. (2). The estimated initial energy fluxes, i. e. $S_{zi}(0)$ value (plasma center) for parabolic using eq. (1) and mean value $\bar{S}_{zi}$, are also shown for comparison.

From Fig. 5, the Poynting vector for the $m = 1$ case gradually decreases with the z axis location (at least, $S_z(0)$ at $z = -2.5$ cm is close to the value of the upper symbol because a standing wave component decreases). For the $m = -1$ case, a strong damping near the antenna region is observed, and we may take the region near the lower symbol at the antenna region due to the dominant formation of the standing wave, which is composed of two waves with the same amplitudes, propagating to the positive and negative z directions, oppositely. This strong damping is mainly due to the higher collisional damping rate, since n_e (electron temperature T_e) near the antenna region is higher (lower) for the $m = -1$ case than that for the $m = 1$ case by about two times (≤ 1.5 times). The obtained axial profiles of n_e and T_e for $m = 1$ and -1 excitations are qualitatively consistent with the axial profile of the ion saturation current.[9] The reason why the localized and higher n_e for the $m = -1$ case than that for the $m = 1$ case is obtained, may be considered as follows. The more peaked power deposition profile is expected for $m = -1$ excitation[5,6] and is consistent with the experimental obtained more peaked n_e profile.[9] Therefore, the experimental results can be explained by the "cooperation effect" since the peaked n_e profile makes the power deposition profile more peaked, which contributes to the higher n_e production near the plasma center for $m = -1$ excitation. The $S_z(0)$ value estimated from eq. (1) at $z = 23$ cm agrees with that from eq. (2) within a factor of 1.5, which means that an approximate estimation of $S_z(0)$ is possible with the use of eq. (1), even if no wave damping is assumed. This also means that the more general expression of eq. (2) can be used for realistic data. From the obtained axial $S_z(0)$ profiles and estimated S_{zi} values, it can be said that we have succeeded for the first time in estimating the Poynting vector by magnetic probe measurements in two ways.

In conclusion, we have distinguished two phases during plasma establishment by applying RF waves: 1) a standing wave before the density jump, and 2) by changing the polarity of the axial magnetic field, the $m = 1$ and $m = -1$ modes of the helicon wave are clearly identified

(through a transient phase) after the jump, measured by the radial excited wave profiles. The energy flux profiles along the cylindrical axis have been estimated for the first time and different profiles were found for the two modes.

1) R. W. Boswell: Plasma Phys. Control. Fusion **26** (1984) 1147.
2) F. F. Chen: Plasma Phys. Control. Fusion **33** (1991) 339.
3) A. Komori, T. Shoji, K. Miyamoto, J. Kawai and Y. Kawai: Phys. Fluids **B3** (1991) 893.
4) P. K. Lowenhardt, B. D. Blackwell, R. W. Boswell, G. D. Conway and S. M. Hamburger: Phys. Rev. Lett. **67** (1991) 2792.
5) T. Shoji, Y. Sakawa, S. Nakazawa, K. Kadota and T. Sato: Plasma Sources Sci. & Technol. **2** (1993) 5.
6) F. F. Chen, M. J. Hsieh and M. Light: Plasma Sources Sci. & Technol. **3** (1994) 49.
7) Y. Yasaka and Y. Hara: Jpn. J. Appl. Phys. **33** (1994) 5950.
8) M. Light and F. F. Chen: Phys. Plasmas **2** (1995) 1084.
9) S. Shinohara, Y. Miyauchi and Y. Kawai: Plasma Phys. Control. Fusion **37** (1995) 1015.
10) S. Shinohara and Y. Kawai: Jpn. J. Appl. Phys. **34** (1995) L1571.